Direct Observation of the Budding and Fusion of an Enveloped Virus by Video Microscopy of Viable Cells

Thomas Bächi

Institute for Immunology and Virology, University of Zürich, CH-8028 Zürich, Switzerland

Abstract. Video-enhanced microscopy and digital image processing were used to observe the assembly, budding, and fusion of Respiratory Syncytial virus. Viral filaments were seen to bud from the plasma membrane of viable infected cells to a final length of 5–10 μm with an average speed of elongation of 110–250 nm/s. The rapidity of viral assembly and its synchronous occurrence (leading to the production of several viral particles per minute from the same surface domain) suggests a directed process of recruitment of viral components to an area selected for virus maturation. Virions were also seen to adsorb to the cell surface, and to fuse with the plasma membrane. These are the first real time observations of viral morphogenesis and penetration which are crucial events in the infectious cycle of enveloped viruses.

THE final step in the maturation of enveloped animal viruses entails the budding of the viral nucleocapsid core through the plasma membrane of the host cell. In reverse (fusion of viral and cellular membranes), this process introduces nucleocapsids into the cytoplasm of susceptible cells and initiates the infectious cycle (White et al., 1983). Previous studies have largely been limited by available techniques to examination of nonviable, fixed material. This has precluded precise determination of the dynamics of budding and fusion, and has prohibited experimental manipulation at the level of individual cells.

In the present study, a high resolution television camera and real time image processing have been used in conjunction with differential interference contrast optics (DIC)[1] to examine the budding and fusion of individual virions from viable, virus-infected cells. In various systems this method has enabled the identification of structures smaller than the theoretical limit of resolution of conventional light microscopy (Allen et al., 1981, 1985; Goldberg and Burmeister, 1986; Vale et al., 1985; Weiss, 1986). Analysis was further facilitated by the use of Respiratory Syncytial (RS) virus, which, when grown in tissue culture, maintains a filamentous morphology easily differentiated from host cell structures (Bächi and Howe, 1973; Berthiaume et al., 1974; Faulkner et al., 1976, Joncas et al., 1969). Using this system, precise information has been obtained for the first time regarding the rates at which viral budding and fusion proceed.

Materials and Methods

Cells

African green monkey kidney (*Vero*) cells were grown in MEM containing 10% FCS. Before infection, cells were washed with Earle's balanced salt solution (EBSS). After inoculation with virus, cells were maintained in MEM containing 2% FCS. For microscopy, cells were grown at subconfluent density on glass cover slips (20 × 27 mm) in six-well plates.

Virus

RS virus (originally obtained from the American Type Culture Collection, Rockville, MD) was maintained by passage in Vero cells as previously described (Bächi and Howe, 1974; Fuchs and Bächi, 1975). For comparison, a wild-type virus from a fresh human isolate (generous gift of Dr. W. Wunderli, University of Zürich), was also used in some experiments and was found to produce morphologically and immunologically identical results.

Antibodies

Monoclonal antibodies (mAbs) specific for G protein of RS virus (Pothier et al., 1985) were obtained from Biosoft (Paris, France). Anti-murine IgG conjugated to TRITC was obtained from Cappel Laboratories, Malverne, PA. Indirect immunofluorescence was performed as described (Bächi et al., 1985).

Microscopy and Image Analysis

For light microscopy, cover slip cultures were mounted with serum-free EBSS and sealed with paraffin onto a glass slide with a spacer frame cut from parafilm. Slides were incubated for at least 15 min at 37°C before their examination in the microscope at a room temperature of 30°C. Immunofluorescence assays were performed using cover slips which had been fixed for 15 min at room temperatures with paraformaldehyde (3% wt/vol). Specimens were examined with a Reichert Polyvar microscope equipped with optics for epifluorescence and Nomarski DIC. Observations were made with oil immersion of both condenser and objective (planapochromate, 100×, 1.32 N.A.). Illumination for both epifluorescence and DIC was provided by a 200-W mercury arc lamp filtered through reflection heat filters (model KG1; Schott Glass Technologies, Inc., Duryea, PA) placed in front of the mercury arc lamp and of the illumination aperture.

Video microscopy (Inoué, 1986) was performed using a Hamamatsu type C 1966-12 SIT camera for epifluorescence microscopy and a Hamamatsu type C-1966-01 chalnicon camera for DIC microscopy. Signals were processed by a computer system (model C1966; Hamamatsu Corp., Middlesex, NJ) as described previously (Allen et al., 1981; Weiss, 1986). Processed images were recorded in real time by a U-matic video cassette recorder

1. *Abbreviations used in this paper*: DIC, differential interference contrast optics; p.i., postinfection; RS, Respiratory Synctial.

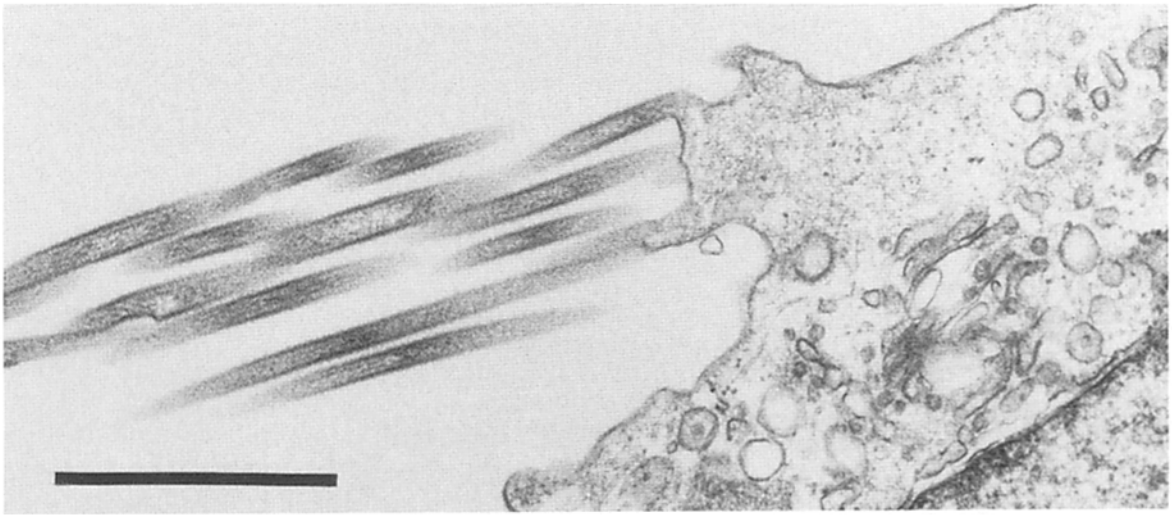

Figure 1. Virus filaments budding of a host cell surface. Vero cell 24 h p.i. reveals an abundance of cell-associated RS virus filaments with a diameter of 100–120 nm at various stages of budding from the host plasma membrane. Note the close association of parallel filaments and the similarity of this pattern to that seen by immunofluorescence (Figs. 2 and 3). Bar, 1 μm.

(Sony, Tokyo, Japan; model VO-5800PS) and/or displayed on a high resolution 7" flat screen monitor (type VM 1710; Lucius & Baer, Federal Republic of Germany) equipped with a photoframe for 35-mm photography. For quanitative analysis of viral filament maturation and release, video recordings of budding events were fed into a Video Manipulator (model C2117, Hamamatsu Corp.) which can be used in an interactive manner to track particle movement and automatically computes average velocity and path lengths. Image magnification was calibrated with an e.m. grid containing a carbon-grating replica with 30,000 lines per inch.

Electron microscopy was performed using a Philips EM 400 electron microscope on ultrathin sections of virus infected cells prepared as previously described (Bächi and Howe, 1973).

Results

Characterization of Viral Filaments

24–48 h postinfection (p.i.) with RS virus, monolayers of Vero cells reveal the typical cytopathic effect of syncytia formation. At the time, parallel arrays of virus filaments of 110 nm diam were easily detected in thin sections of infected cells by electron microscopy (Fig. 1). Similar arrays of filaments could be visualized on the surface of paraformaldehyde fixed cells by DIC microscopy (Fig. 2 *b*). Fine adjustment of focus revealed most of the filaments to be on the surface of cells facing the glass substrate (Figs. 2 *a* and 3 *a*). Virus budding from peripheral areas of cells demonstrated in a more randomized arrangement of filaments (Fig. 3 *d*). Although some free filaments which seemed to be attached to the cover slip were observed, it was apparent that virus tended to accumulate on the cell surface rather than being completely released after budding.

Indirect immunofluorescence using mAbs specific for the major RS virus glycoprotein and TRITC-conjugated anti-

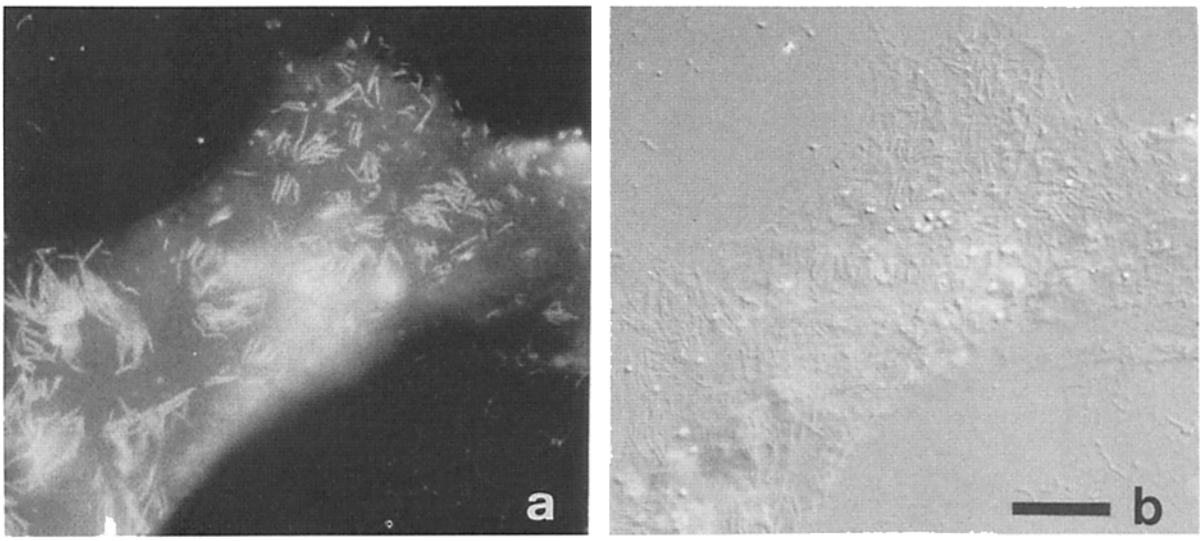

Figure 2. Surface immunofluorescence and DIC microscopy of cells infected with RS virus. Cells 24 h p.i. and labeled with anti-G mAb and anti-mouse IgG-TRITC visualized with conventional immunofluorescence photography reveal the presence of intensely stained viral filaments which remain associated with a weakly fluorescent host cell surface (*a*). Same area observed with DIC optics permits the detection of filaments and their localization on the basolateral side of the cell (*b*). Bar, 10 μm.

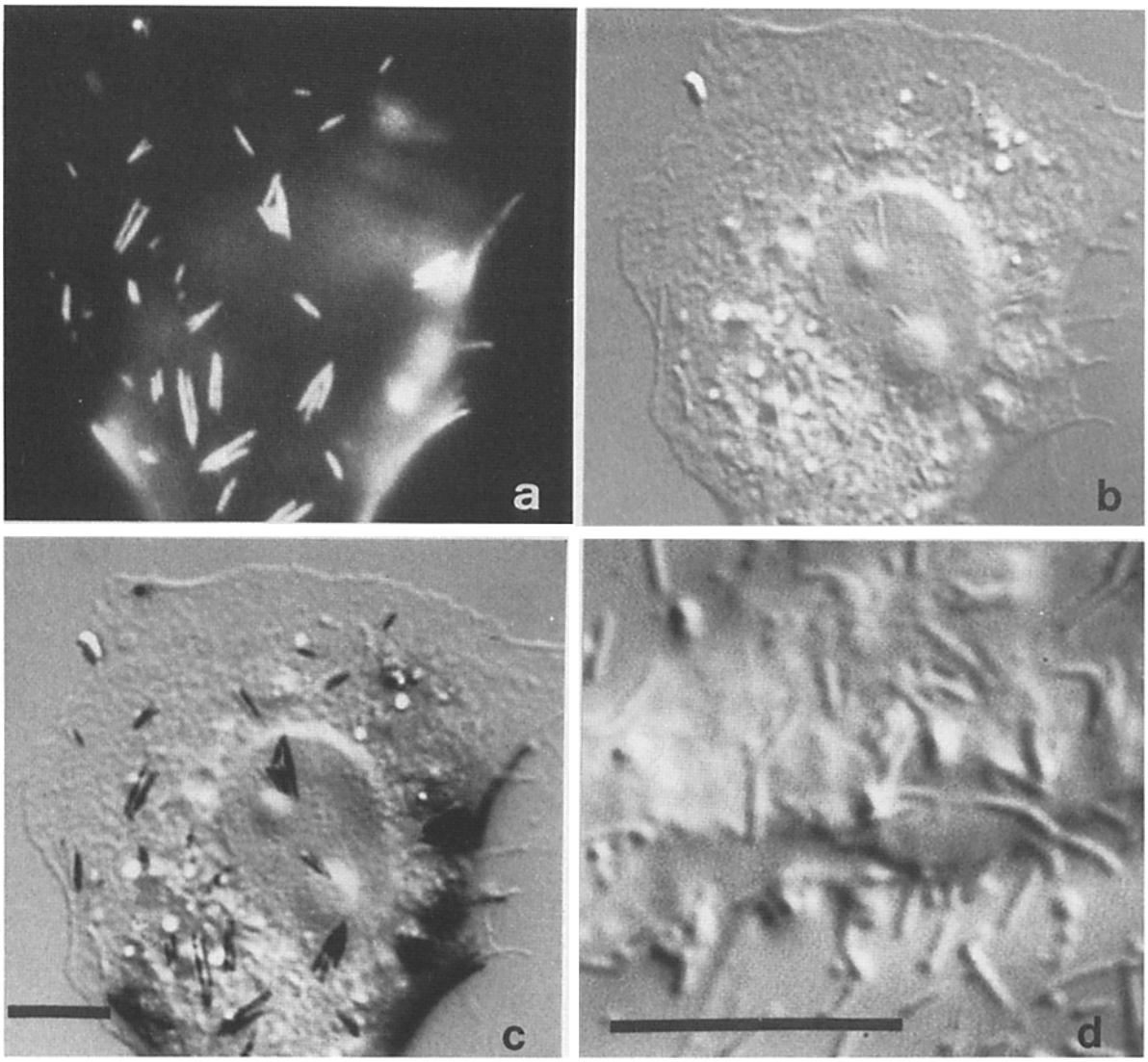

Figure 3. Recognition of RS virus filaments by video microscopy. Vero cell 24 h p.i. fixed for immunofluorescence (same material as Fig. 2) visualized with a SIT camera. Digital processing and storage of the same image in a frame memory (*a*) was used for a subtraction of the identical area imaged with DIC optics (*b*) to produce a composite image (*c*) for colocalization of cellular structures with viral antigens. Observation of viral filaments in living cells with a high resolution Chalnicon camera (*d*) reveals well-defined viral filaments. Bars, 10 μm.

mouse IgG confirmed that filaments consisted of viral antigens (Figs. 2 *a* and 3 *b*). The bright fluorescence of the viral filaments contrasted markedly with the faint fluorescence of the plasma membrane.

The use of video microscopy allowed for digital manipulation of images. Digital subtraction of the fluorescence image (Fig. 3 *a*) from the DIC image (Fig. 3 *b*) of the same field gave a composite image in which fluorescent viral antigens and cellular structures identified by DIC optics clearly colocalized (Fig. 3 *c*). The relatively low resolution of the highly sensitive silicon intensified target camera used to detect immunofluorescence limited the resolution of viral filaments. Resolution was further decreased by paraformaldehyde fixation of the samples which decreased the intrinsic contrast of cellular and viral structures. Images of high resolution and magnification were obtained by using a chalnicon television tube and viable cells maintained in serum-free media (Figs. 3 *d*, 4, and 5).

Real Time Observation of Viral Budding and Fusion

Images were of sufficient quality to observe the budding of virions in real time. Three types of motion could be distinguished in budding viral filaments. First, budding virions demonstrated a high frequency, low displacement vibration which most likely represents Brownian motion. Second, many filaments demonstrated a low frequency, high displacement movement perpendicular to the long axis which increased with filament length. Third, filaments increased in length until the budding process was completed.

The dynamics of filament assembly were documented by still photographs of video recordings of two experiments performed with Vero cells 6 h p.i. (Figs. 4 and 5). The tendency of budding events to cluster into localized areas of the cell meant that observation of any given microscopic field was unlikely to demonstrate active budding within a reasonable period of time. Through experience, however, it was possible to identify promising areas of the cell surface during scan-

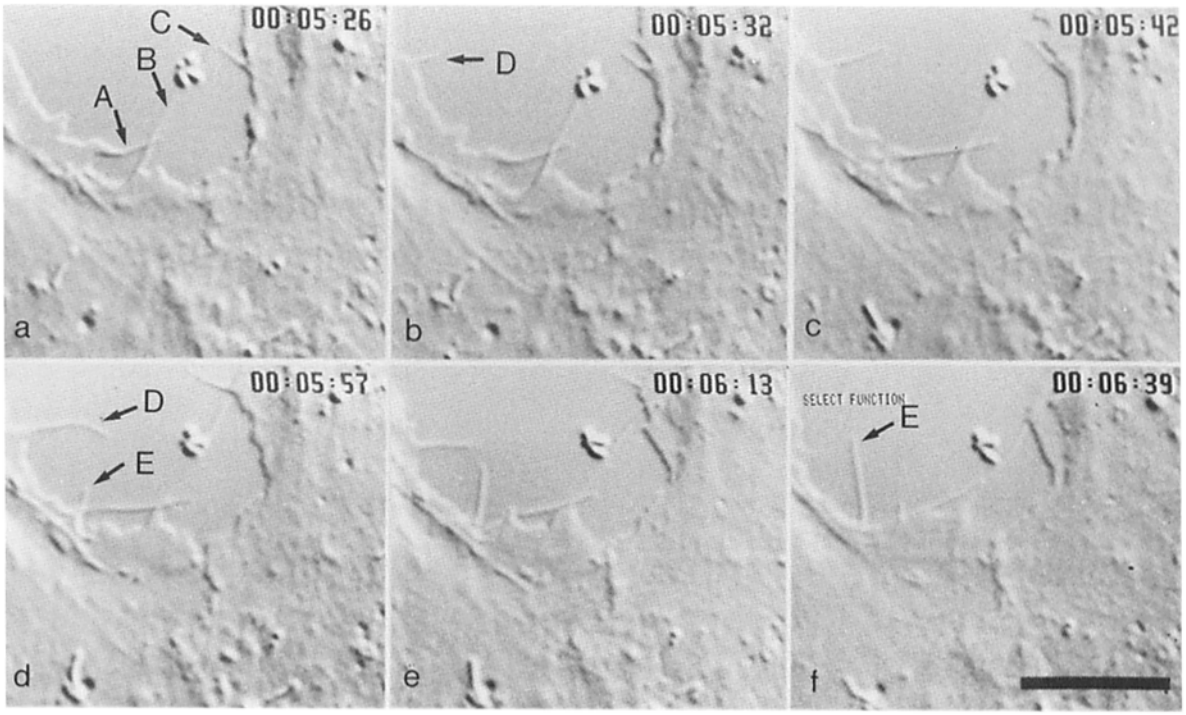

Figure 4. Sequence from a video recording of the assembly of RS virus filaments. Vero cell 6 h p.i. observed over a period of 73 s (timer indicates hours, minutes, and seconds). (*a*) Initially, the periphery of the infected cell reveals several viral filaments (*A*, *B*, and *C*) at various stages of budding. Formation and elongation of new filaments D (*b–e*) and E (*d–f*) occur almost synchronously and within close proximity. Complete tracking and measurement of average speed of growth of all viruses detected in this area is shown in Fig. 7 *a*. Bar, 10 μm.

ning by the occurrence of violent cytoplasmic movements in localized areas of the cell. Fig. 4 depicts events occurring in a 73-s time span in one such area. In the initial frame (Fig. 4 *a*), three filaments can be seen; in later frames (Fig. 4, *b* and *d*) at least two other filaments appear. Each of the filaments lengthened at a rate of ~200 nm/s until attaining a typical length of 5 μm. At this point, filament growth abruptly ended, and in a few cases, the filament suddenly disappeared from the field, which is indicative of filament release from the cell surface (note that the virion may subsequently attach to another area of the cell, other cells, or the glass surface).

Fig. 5 represents a sequence of pictures taken from a video recording of the maturation and later fate of a single virus filament over an observation period of 238 s. At first, budding of the viral filament proceeded during 75 s to produce a filament with a length of ~10 μm (Fig. 5, *a–d*). As with most virions observed in this study, it remained attached to the cell surface by its end despite rapid motions (Fig. 5, *e–g*) which moved the filament into a horizontal position in close proximity to the plasma membrane. This position enabled the filament to adsorb to the cell surface, a phenomenon which was clearly recognized by a complete stop of both the high and low frequency motions of the virus (Fig. 5 *h*). During the following 54 s, the contours of the immobilized virions gradually faded, until they were indiscernible. This latter development is shown again at higher magnification to allow a better appreciation of the process of adsorption (Fig. 6 *a*), and the subsequent disappearance of the filament on the cell surface (Fig. 6 *b*). We interpret this event to represent fusion of a nascent particle with the cell surface. Viral surface fusion events in which, however, the preceeding maturation process escaped direct observation was detected in four more cases (not shown); the average time it took to integrate the total length of the viral filaments into the cell surface was always in the same range as that described in Fig. 5.

To quantitate the rate of filament maturation, video recordings were analyzed with a video manipulator programmed to track movement and calculate velocity (Fig. 7, Table I). Eleven filaments detected over a period of 245 s in the field shown in Fig. 4, displayed an average growth rate of 244 nm/s. The complete maturation of an individual filament was monitored at sampling intervals of 5 s over a period of 37 s; this revealed a similar average velocity of 224 nm/s with a SD of 44.7 nm/s (Fig. 7 *b*). The high value of the SD for this sample reflects the fact that the initial velocity of growth filaments is generally greater than the velocity as budding is completed. Average growth speeds varied from one experiment to another within a range of 100 to 300 nm/s; elongation of viral filaments occurred, however, at remarkably uniform rates within a given experiment (Table I).

Discussion

Video microscopy of viable RS virus–infected cells has enabled for the first time direct observation of the budding and fusion of an enveloped virus. The filamentous morphology of RS virus (Norrby et al., 1970; Bächi and Howe, 1973; Faulkner et al., 1976) proved particularly useful for this analysis. The viral nature of the filaments observed in the present study was readily demonstrated by the perfect correlation of their morphology and arrangement in DIC micros-

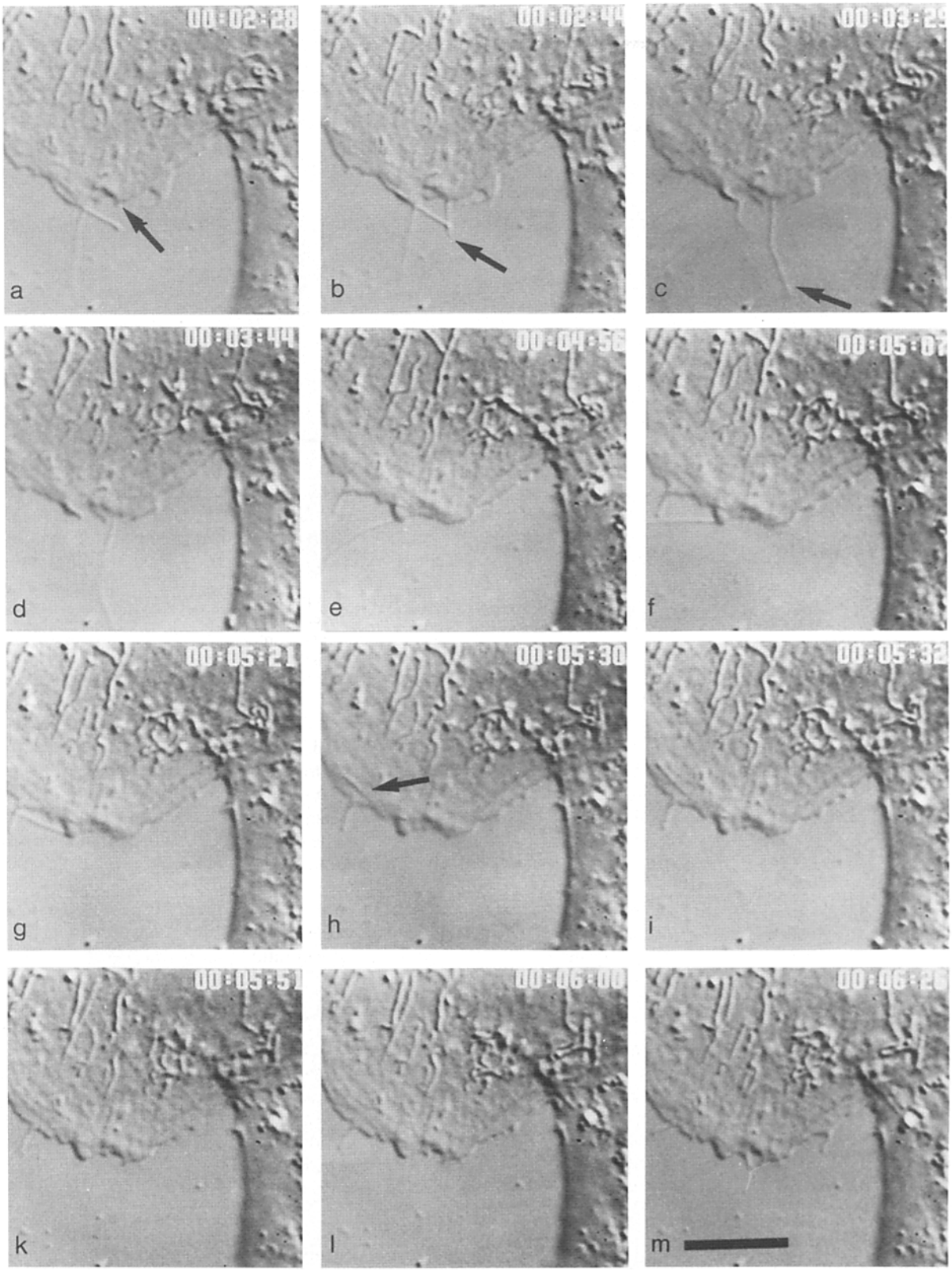

Figure 5. Sequence from a video recording of the assembly, adsorption, and fusion of RS virus. *Vero* cell 6 h p.i. observed over a period of 238 s. Beginning of assembly (*arrow* in *a*) is followed by a constant elongation of the filament (*b* and *c*) until it reaches a final length of 10 μm (*d*). After failure of the virus to be released from the cell, vigorous motions in addition to Brownian motions displace the filament (*e–g*). Adsorption of the filament to the cell surface is signaled by its sudden immobilization (*arrow* in *h*) which is followed by a gradual disappearance as a result of fusion with the plasma membrane (cf. Fig. 6) within 54 s (*i–m*). Bar, 10 μm.

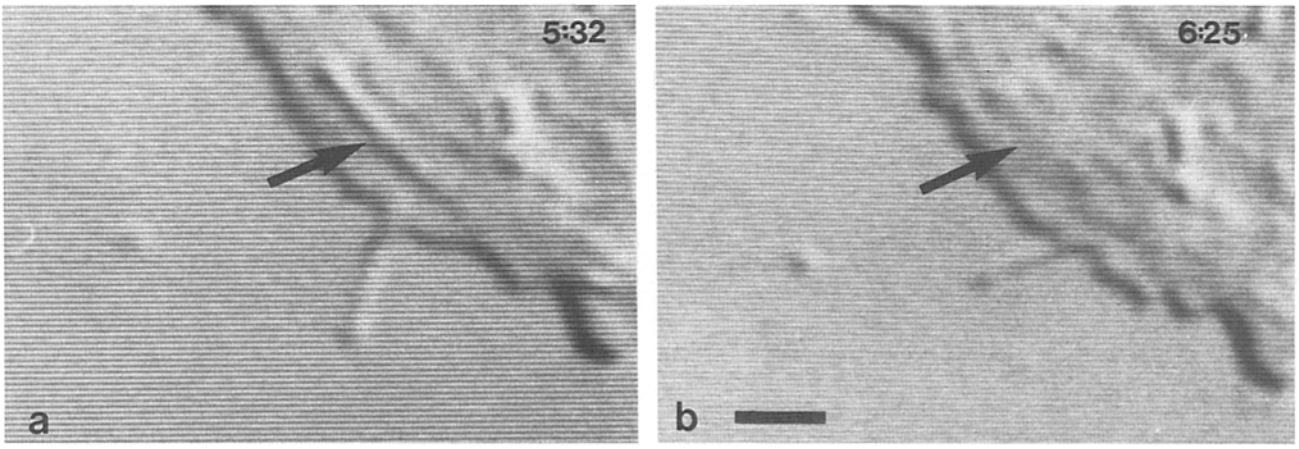

Figure 6. Details from Fig. 5 at higher magnification showing the virus filament at the moment of adsorption to the cell surface (*a*), and after completion of its fusion with the plasma membrane (*b*). Bar, 2 μm.

copy (Figs. 3–5) with the forms detected by immunofluorescence (Figs. 2 and 3) and electron microscopy (Fig. 1).

The rate of virus filament elongation which is a direct illustration of the process of viral assembly occurred with an average speed of 110–250 nm/s. This value depends on a number of parameters whose influence on the process of viral assembly requires more detailed analysis. Observations in the present study were made at a room temperature of ~30°C; it is possible that the process occurs even more rapidly at 37°C. The effect of temperature, pH, stage of infection on the rate of budding is an area of future investigation. It should be possible to examine the generality of the values determined with RS virus by using present methodology to study budding of other filamentous viruses, among which primary isolates of influenza viruses may be the most prominent example (Hoyle, 1950; Burnet et al., 1957; Kilbourne et al., 1960). It remains to be determined whether this method will be useful for studying the maturation of spherical virions, which have a typical diameter of 150 nm. If maturation occurs at a similar rate as RS virus filaments, the process of budding would be completed in <2 s. This, in conjunction with their small size, might preclude direct observation of budding.

It is intriguing that maturation of virions occurs within circumscribed regions of the cell surface overlaying regions of cytoplasm undergoing hectic motion. This could reflect clustering of glycoprotein spikes or internal capsid components at selected areas of the plasma membrane. Alternatively, areas of the plasma membrane may selectively be induced to incorporate viral components evenly distributed at the cell surface. Once budding is completed, many virions fail to detach from the plasma membrane. This is consistent with the

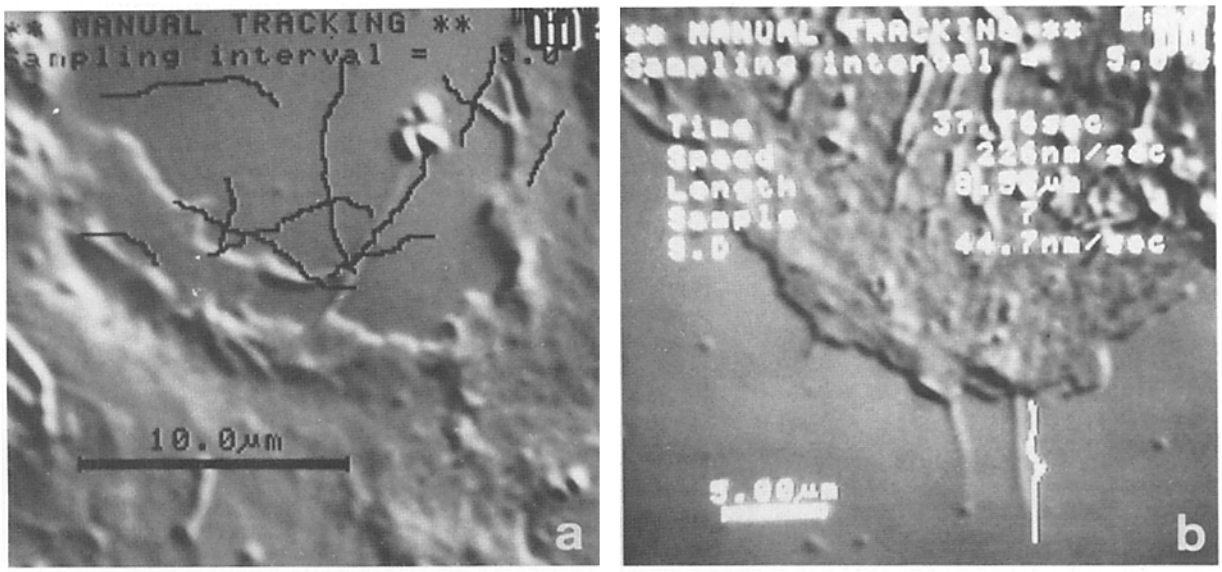

Figure 7. Quantitative analysis of the video recordings documented in Figs. 4 and 5 by interactive tracking of viral budding events. (*a*) Growth paths (total length: 70 μm) of 11 virus filaments which were detected within a time period of 245 s and which grew at an average speed of 253 nm/s. Same field of view as Fig. 4. (*b*) Growth track of virus described in Fig. 5 over a length of 9.49 μm at an average speed of 224 nm/s.

Table I. Determination of Virus Filament Growth Speed

Field of observation	No. of viruses	Average speed	SD	Method of measurement
		nm/s		
Fig. 7 *a*	11	253	39.3	a
Fig. 7 *b*	1	224	44.7	b
Not shown	3	115	10.1	a

Average speed within a population of viruses was determined by manual tracking during 5–10 s per filament (method *a*); average speed of an individual filament was determined by tracking the entire budding process with sampling intervals of 5 s (method *b*). The three fields of observation represent three different experiments of Vero cells infected with RS virus.

fact that up to 90% of the infectivity of RS virus propagated in vitro is cell associated (Levine and Hamilton, 1969). The numerous virus particles detected between the glass surface and the face of the cell contacting the substrate may represent either undissociated or trapped filaments. It remains to be determined whether, in analogy to other viruses which preferentially mature from apical or basolateral surfaces of polarized epithelial cells, this is due to the polarized expression of the viral integral membrane proteins.

In a few instances it was possible to observe the incestuous fusion of a nascent virion with its host cell. Assuming that fusion occurred in a linear fashion (as opposed to the establishment of multiple, interconnecting membrane bridges which could not be detected), the time it took to integrate an entire filament with a cell surface (54 s for 10 μm in Fig. 5 suggests an average speed of 188 nm/s) always occurred at a striklingly similar rate as that determined for the process of budding. This could indicate that membrane budding and fusion depend on common parameters controlling the flow of membranes. Even though the ability of RS virus to fuse to the plasma membrane has also been documented by electron microscopy (Howe et al., 1974), the understanding of the relationship of this type of interaction with the mechanism used by the virus for its infectious entry into cells remains to be further established by biochemical analysis. It is important to emphasize that despite the fact that most mature RS virions remained associated with cells, fusion occurred only rarely. This, of course, is useful strategy for virus reproduction since reinfection would not be expected to increase the yield of virions. It is unclear however how the virus distinguishes infected cells from uninfected cells. There are two solutions to this problem. First, the virus may not actually distinguish infected from uninfected cells, and fusion may simply occur at low frequency after adsorption. Second, the surfaces of uninfected and infected cells may differ. This could reflect the action of viral gene products which alter cellular receptors; many members of the paramyxovirus family possess such receptor destroying activity.

In conclusion, video microscopy of viable RS virus–infected cells has allowed the direct observation in real time of a variety of virus-host cells interactions (adsorption, fusion, budding) critical to life cycle of enveloped viruses. This method enables examination of the maturation and entry of individual virions, opening new avenues for research which should add to our knowledge of virus-host interactions.

I would like to thank Ruth Keller for her excellent technical assistance, and Dr. J. Yewdell for his help with the manuscript.

Part of the video equipment was purchased with a support from the Hartmann-Müller Foundation, Zürich.

Received for publication 21 October 1987, and in revised form 5 July 1988.

References

Allen, R. D., N. S. Allen, and J. L. Travis. 1981. Video-enhanced contrast, differential interference contrast (AVEC-DIC) microscopy: a new method capable of analyzing microtubule-related motility in the reticulopodial network of allogromia laticollaris. *Cell Motil.* 1:291–302.

Allen, R. D., D. G. Weiss, J. H. Hayden, D. T. Brown, H. Fujiwake, and M. Simpson. 1985. Gliding movement of and bidirectional transport along single native microtubules from squid axoplasm: evidence for an active role of microtubules in cytoplasmic transport. *J. Cell Biol.* 100:1736–1752.

Bächi, T., and C. Howe. 1973. Morphogenesis and ultrastructure of respiratory syncytial virus. *J. Virol.* 12:1173–1180.

Bächi, T., W. Gerhard, and J. Yewdell. 1985. Monoclonal antibodies detect different forms of influenza virus hemagglutinin during viral penetration and biosynthesis. *J. Virol.* 55:307–313.

Berthiaume, L., J. Joncas, and V. Pavilanis. 1974. Comparative structure, morphogenesis and biological characteristics of the respiratory syncytial (RS) virus and the pneumonia of mice. *Arch. ges. Virusforsch.* 45:39–51.

Burnet, F. M., and P. E. Lind. 1957. Studies on filamentary forms of influenza virus with special reference to the use of dark-ground microscopy. *Arch. ges. Virusforsch.* 7:413–428.

Faulkner, G. P., P. V. Shirodaria, E. A. C. Follett, and C. R. Pringle. 1976. Respiratory syncytial virus ts mutants and nuclear immunofluorescence. *J. Virol.* 20:487–500.

Fuchs, H., and T. Bächi. 1975. Scanning electron microscopical demonstration of respiratory syncytial virus antigens by immunological markers. *J. Ultrastruct. Res.* 52:114–119.

Goldberg, D., and D. W. Burmeister. 1986. Stages in axon formation: observation of growth of axons in culture using video-enhanced contrast-differential interference contrast microscopy. *Cell.* 103:1921–1931.

Howe, C., T. Bächi, and K. C. Hsu. 1974. Application of immunoferritin techniques for the detection of viral and cellular antigens. *In* Viral Immunodiagnosis. E. Kurstak, and R. Modisset, editors. Academic Press, New York. 215–234.

Hoyle, L. 1950. The multiplication of influenza viruses in the fertile egg. *J. Hyg.* 48:277–297.

Inoué, S. 1986. Video microscopy. Plenum Press, New York. 1–584.

Joncas, J., L. Berthiaume and V. Pavilanis. 1969. The structure of respiratory syncytial virus. *Virology.* 38:493–496.

Kilbourne, E. D., and J. S. Murphy. 1960. Genetic studies of influenza viruses. I. Viral morphology and growth capacity as exchangeable genetic traits. Rapid in ovo adaptation of early passage asia strain isolates by combination with PR8. *J. Exp. Med.* 111:387–405.

Levine, S., and R. Hamilton. 1969. Kinetics of the respiratory syncytial virus growth cycle in HeLa cells. *Arch. ges. Virusforsch.* 28:122–132.

Norrby, E., H. Marusyk, and C. Örvell. 1970. Morphogenesis of respiratory syncytial virus in a green monkey kidney cell line (Vero). *J. Virol.* 6: 237–242.

Pothier, P., J. C. Nicolas, G. Prudhomme de Saint Maur, G., S. Ghim, A. Kazmierczak, and F. Bricout. 1985. Monoclonal antibodies against respiratory syncytial virus and their use for rapid detection of virus in nasopharyngeal secretions. *J. Clin. Microbiol.* 21:286–287.

Vale, R. D., B. J. Schnapp, T. S. Reese, and M. P. Sheetz. 1985. Movement of organelles along filaments dissociated from the axoplasm of the squid giant axon. *Cell.* 40:449–454.

Weiss, D. G. 1986. Visualization of the living cytoskeleton by video-enhanced microscopy and digital image processing. *J. Cell Sci.* 5(Suppl.):1–15.

White, J., M. Kielian, and A. Helenius. 1983. Membrane fusion proteins of enveloped animal viruses. *Quart. Rev. Biophys.* 16:151–195.